OPEN

Immune-related signature identifies IL1R2 as an immunological and prognostic biomarker in pancreatic cancer

Chengcheng Wang[a,b,c,d], Yuan Chen[a,c,e], Xinpeng Yin[a,c,e], Ruiyuan Xu[a,c,e], Rexiati Ruze[a,c,e], Jianlu Song[a,c,e], Chenglin Hu[a,c,e], Yupei Zhao[a,b,c,e,*]

Abstract

Objective: Pancreatic cancer is one of the most aggressive malignancies, a robust prognostic signature and novel biomarkers are urgently needed for accurate stratification of the patients and optimization of clinical decision-making.

Methods: A list of bioinformatic analysis were applied in public dataset to construct an immune-related signature. Furthermore, the most pivotal gene in the signature was identified. The potential mechanism of the core gene function was revealed through GSEA, CIBERSORT, ESTIMATE, immunophenoscore (IPS) algorithm, single-cell analysis, and functional experiment.

Results: An immune-related prognostic signature and associated nomogram were constructed and validated. Among the genes constituting the signature, interleukin 1 receptor type II (IL1R2) was identified as the gene occupying the most paramount position in the risk signature. Meanwhile, knockdown of IL1R2 significantly inhibited the proliferation, invasion, and migration ability of pancreatic cancer cells. Additionally, high IL1R2 expression was associated with reduced CD8+ T cell infiltration in pancreatic cancer microenvironment, which may be due to high programmed cell death-ligand-1 (PD-L1) expression in cancer cells. Finally, the IPS algorithm proved that patients with high IL1R2 expression possessed a higher tumor mutation burden and a higher probability of benefiting from immunotherapy.

Conclusion: In conclusion, our study constructed an efficient immune-related prognostic signature and identified the key role of IL1R2 in the development of pancreatic cancer, as well as its potential to serve as a biomarker for immunotherapy efficacy prediction for pancreatic cancer.

Keywords: CD8+ T cells, IL1R2, Immunotherapy, Pancreatic cancer, Tumor microenvironment

Introduction

Pancreatic cancer (PC) is one of the most malignant tumor with a 5-year survival rate of only 12%.[1] Meanwhile, according to the latest epidemiological data, the global burden of PC has increased dramatically over the past few decades and is expected to become a leading cause of cancer-related mortality.[2] The poor prognosis of PC is mainly due to the lack of sensitive screening methods, remarkable resistance to most conventional treatment options, and complex tumor microenvironments.[3] Apart from that, the lack of accurate predictive signature and effective therapeutic targets is also a contributor of the dismal status.[4,5] Therefore, it is of great significance to construct accurate prognostic signature of PC and identify potential key factors determining the oncogenesis and development of PC.

The immunological components within tumors, termed the tumor immune microenvironment (TIME), has been proved to be strongly related to cancer development.[6,7] Gao et al[8] has reported that tumor-derived ILT4/PIR-B was directly involved in induction of cell senescence in naive/effector T cells mediated by tumor cells in vitro and in vivo, which contributed to the progression of the tumor. Meanwhile, OTU deubiquitinase 5 (OTUD5)-mediated deubiquitination of yes-associated protein (YAP) in macrophage promoted M2 phenotype polarization and favored triple-negative breast cancer progression.[9] Therefore, an immune-related prognostic signature was considered to accurately predict the prognosis of PC patients. Furthermore, the most paramount gene in the risk signature was further explored, as well as its potential mechanisms and ability to serve as a novel biomarker for predicting the efficiency of immunotherapy.

In the present study, an immune-related prognostic signature and associated nomogram were constructed and validated. Among the genes constituting the signature, interleukin 1 receptor type II (IL1R2) was identified as the gene occupying the most paramount position in the risk signature, which was strongly associated with poor prognosis of PC patients. Meanwhile, knockdown of IL1R2 in PC cells resulted in a significant decrease of the proliferation, invasion, and migration ability. CIBERSORT, ESTIMATE, and Gene Set Enrichment Analysis (GSEA) algorithms illustrated a lower CD8+ T cell

[a]Key Laboratory of Research in Pancreatic Tumor, Chinese Academy of Medical Sciences, Beijing 100023, P.R. China, [b]National Infrastructures for Translational Medicine, Peking Union Medical College Hospital, Beijing 100023, P.R. China, [c]State Key Laboratory of Complex, Severe, and Rare Diseases, Peking Union Medical College Hospital, Chinese Academy of Medical Science and Peking Union Medical College, Beijing 100023, P.R. China, [d]Institute of Clinical Medicine, Peking Union Medical College Hospital, Beijing 100023, P.R. China, [e]Department of General Surgery, Peking Union Medical College Hospital, Peking Union Medical College, Chinese Academy of Medical Sciences, Beijing 100023, P.R. China

CW and YC contributed equally to this article.

Supplemental digital content is available for this article.

The datasets used and/or analyzed during the current study are available from the corresponding author on reasonable request.

* Corresponding author: Yupei Zhao, Key Laboratory of Research in Pancreatic Tumor, Chinese Academy of Medical Sciences, Beijing 100023, P.R. China. E-mail: zhao8028@263.net

infiltration in patients with high IL1R2 expression, which was associated with high programmed cell death-ligand-1 (PD-L1) expression in IL1R2 high expression PC cells. In addition, single-cell analysis confirmed the difference in the interaction with T cells between IL1R2-high and IL1R2-low expression cancer cells and demonstrated a lower percentage of CD8+ T cells in patients with high IL1R2 expression. Finally, the immunophenoscore (IPS) algorithm demonstrated that patients with high IL1R2 expression possessed a higher tumor mutation burden (TMB) and better responsiveness to immunotherapy, suggesting that IL1R2 was expected to be a potential biomarker for predicting PC immunotherapy efficiency.

Methods

Datasets sources and processing

Immune-related genes (IRGs) were extracted and integrated from the ImmPort database (https://immport.niaid.nih.gov; March 1, 2021)[10] (Additional Table S1, http://links.lww.com/JP9/A53). Genomics data and clinical information were downloaded from The Cancer Genome Atlas (TCGA) dataset (https://portal.gdc.cancer.gov/; March 1, 2021). Samples with inadequate clinical information and follow-up period less than 30 days were excluded. Finally, 166 cases were included in the study (Additional Table S2, http://links.lww.com/JP9/A54). Log2(TPM+0.01) was used throughout the analysis unless otherwise noted.

In addition, GSE62452, GSE78229, and GSE71729 dataset were downloaded from Gene Expression Omnibus (GEO) (http://www.ncbi.nlm.nih.gov/geo/).[11–13] The normalized expression matrix of microarray data can be directly download from the GEO. Probes were then matched to the gene symbols using the annotation files provided by the manufacturer. Furthermore, the single-cell dataset CRA001160 was downloaded from Tumor Immune Single-cell Hub (TISCH) database (http://tisch.comp-genomics.org/).[14,15] And the RNA-seq data of all pancreatic cell lines was extracted from the Cancer Cell Line Encyclopedia (CCLE) database.[16]

Establishment of the prognostic signature and nomogram based on IRGs

Limma package was applied to analyze differentially expressed genes (DEGs) in GSE71729 and GSE62452.[17] |Fold change| >1.5 and false discovery rate (FDR) <0.05 were set as the cutoffs for the DEGs. The intersection of differential genes was further selected by univariate Cox regression analysis, least absolute shrinkage and selection operator (LASSO) regression analysis and multivariate Cox regression analysis to construct the optimal prognosis signature of PC. The risk score of the signature was calculated as follows: risk score = (exprgene1 × Coefgene1) + (exprgene2 × Coefgene2) + … + (exprgenen × Coefgenen). Subsequently, the nomogram based on the gene signature and clinicopathological factors was also established to predict the 1.0-, 1.5-, 2.0-year survival probability of PC patients.

Gene Set Enrichment Analysis

Patients in the TCGA entire set were divided into IL1R2 high expression group and IL1R2 low expression group, followed by DEGs analysis and GSEA. The ALL ontology of the genes was analyzed by Gene Ontology (GO),[18] while pathway enrichment was analyzed by the Kyoto Encyclopedia of Genes and Genomes (KEGG).[19] The number of random sample permutations was set at 1000, and nominal (NOM) P value <.05 and FDR q value <0.25 were set as the significance threshold.

TIME analysis, TMB calculation, and immunotherapy efficacy prediction

The CIBERSORT algorithm was used to calculate the proportion of 22 types of immune cells in each patient's tumor microenvironment, while the ESTIMATE algorithm was applied to score the immune infiltration in the patient's tumor microenvironment.[20,21] The mutation profile of each patient was acquired from TCGA data portal (https://portal.gdc.cancer.gov/; March 1, 2021) and analyzed by "maftools" package.[22] Additionally, IPS algorithm was applied to estimate the probability that PC patients respond to immunotherapy, including anti-PD-1 therapy, anti-CTLA-4 therapy, and the combination of anti-PD-1 and anti-CTLA-4 therapy (https://tcia.at/).[23]

scRNA-seq data quality control, dimension reduction, and cell clustering

The processed expression matrix and clinical information of the single-cell dataset CRA001160 were downloaded from TISCH database and analyzed by Seurat package.[14] Low quality cells (<200 genes/cell, <3 cells/gene, >5% mitochondrial genes, total expressed genes <200, and total expressed genes >7000) were removed. Subsequently, principal component analysis (PCA) was performed and the first 15 dimensions were used to compute a Uniform Manifold Approximation and Projection (UMAP, res = 1.0). In addition, the cell types were annotated according to the markers provided by the author.[15]

Cell culture

The origin and culture of the cells are described in the previous article.[24] In brief, BxPC-3 cell line was cultured in RPMI-1640 medium (Corning, NY, USA, #10–040-CV), and T3M4 cell line was cultured in high glucose Dulbecco Modified Eagle Medium (DMEM; Corning, #10–013-CMR). All medium were supplemented with 10% fetal bovine serum (FBS) (HyClone, UT, USA, #SH30073.03) and 1% Penicillin–Streptomycin (Life Technologies, MA, USA, #15,140–122).

siRNA transient transfection

Small interfering RNA (siRNA) targeting IL1R2 was purchased from Tsingke (Tsingke Biotechnology, Beijing, China). Sequences of siRNAs used were as follows: siIL1R2-1#: 5′-GUAUUGAGCUACGCAUCAA-3′; siIL1R2-2#: 5′-GACUGACAAUCCCGUGUAA-3′. Transfections of each siRNA (80nM) was performed using Lipofectamine 3000 (Invitrogen, Carlsbad, CA) according to the manufacturer's instruction.

Western blot analysis

The specific process of western blot analysis was described previously.[25] The primary antibodies anti-IL1R2 (1:1000, Proteintech, Wuhan, China, 60262-1-Ig), and anti-glyceraldehyde-3-phosphate dehydrogenase (GAPDH) (1:20000; Proteintech, 60004-1-Ig) were used overnight at 4°C and then incubated with horseradish peroxidase (HRP)-conjugated secondary antibodies (1:5000; Proteintech, SA00001-1 and SA00001-2) at room temperature for 1 hour. Chemiluminescence assay (Thermo scientific, MA, USA, 34580) was utilized to visualize protein bands.

RNA extraction and quantitative real-time PCR analysis

The specific operation process has been described in the previous article.[26] The expression of genes was normalized to GAPDH, and the 2-ΔΔCt method was used to quantify the fold change. The primer sequences used for qRT-PCR were as follows:

IL1R2:

Forward 5′-ATGTTGCGCTTGTACGTGTT-3′,

Reverse 5′-CCCGCTTGTAATGCCTCCC-3′;

GAPDH:

Forward 5′-GTCTCCTCTGACTTCAACAGCG-3′,

Reverse 5′-ACCACCCTGTTGCTGTAGCCAA-3′.

Cell proliferation assay

The specific experimental procedure has been described in the previous article.[27] In brief, cancer cells from control and treatment groups were seeded into 96-well plates and measured the optical density (OD) values with Cell Counting Kit-8 (CCK-8) reagent (Dojindo Laboratories, Shanghai, China, CK04) at 0, 24, 48, 72, 96 hours, respectively.

Migration and invasion assay

The specific experimental procedure has been described in the previous article.[28] In brief, 100,000 cells resuspended in 150 μL of serum-free medium were seeded into upper transwell chamber (24-well and 8.0 μm pore size, Corning, 3422) with or without Matrigel (Corning, 354234). And 600 μL of medium containing 10% FBS was added to the lower chamber. The migrated cells were then fixed with methanol and stained after 24 hours of incubation.

Statistical analysis

All statistical analysis was performed in GraphPad Prism 8 (version 8.0.1) and R software (version 4.1.0). Biological replicates are shown as means ± standard error of mean (SEM) of 3 independent experiments. *P* values are specified in figures.

Results

Five IRGs were screened out for constructing the risk signature

First, DEGs analysis was performed on IRGs in GSE71729 and GSE62452 datasets (Fig. 1A, B, |Fold change| >1.5 and FDR < 0.05 were regarded as statistically significant), and 75 DEGs were obtained after taking the intersection (Fig. 1C). Subsequently, univariate cox analysis was conducted to screen the prognosis-related genes, and LAASO regression analysis was
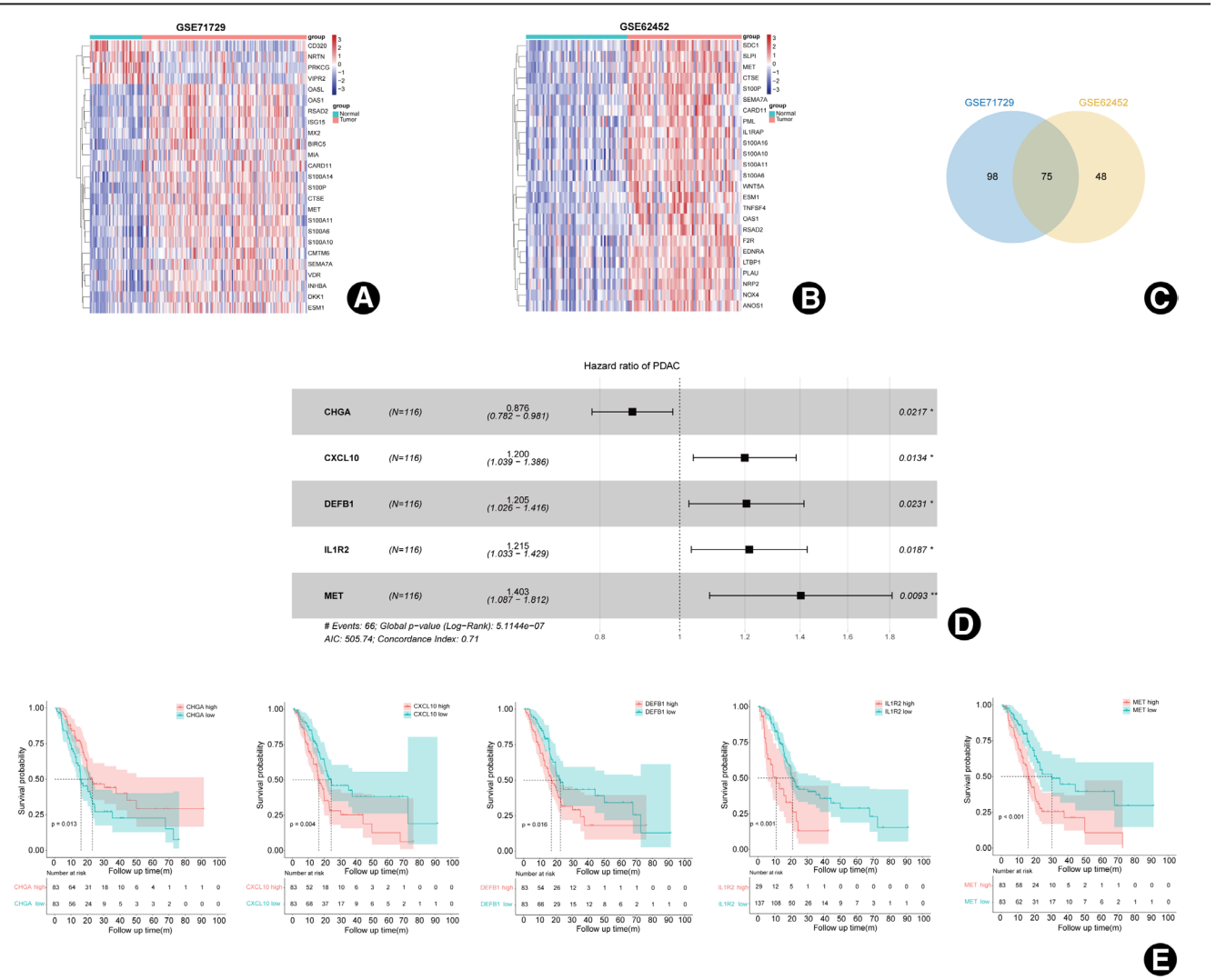
Figure 1. Screening out immune-related genes for risk signature construction. (A, B) Heatmap of immune-related DEGs between normal tissue and PC in GSE71729 and GSE62452. (C) Venn plot of the intersection of 2 DEGs datasets. (D) Five IRGs were screened out for constructing a risk signature. (E) Kaplan-Meier analysis of the 5 genes in the risk signature. AIC = Akaike information criterion, DEG = differentially expressed gene, IRG = immune-related gene, PC = pancreatic cancer, PDAC = pancreatic ductal adenocarcinoma.

applied to avoid overfitting problems and further screen the candidate genes (Additional Figure S1A, B, http://links.lww.com/JP9/A51, log(lambda.min) = −2.876043). Finally, multivariate Cox analysis was then used to explore an optimal gene combination for establishing the risk signature for PC patients (Fig. 1D), which outputted a prognostic signature for PC consisting of 5 IRGs (CHGA, CXCL10, DEFB1, IL1R2, MET). Among them, CXCL10, DEFB1, IL1R2, and MET were risk factors for PC, while CHGA was a protective factor for PC (Fig. 1E).

Validation of the signature for predicting prognosis of PC patients

To further evaluate the validity of the prediction signature, we calculated the risk score for each patient separately based on their gene expression profiles (risk score = (−0.1324 × expression level of CHGA) + (0.1820 × expression level of CXCL10) + (0.1867 × expression level of DEFB1) + (0.1946 × expression level of IL1R2) + (0.3389 × expression level of MET)). And the effectiveness of the signature was validated in the TCGA training set, TCGA testing set, TCGA entire set, and GSE78229 dataset by combining analysis of their clinical information (Fig. 2A).

Based on the results of Kaplan-Meier (K-M) curve analysis, it was found that the prognosis of patients in the high-risk group was significantly worse than those in the low-risk group (Fig. 2B–E, $P < .05$ in TCGA training set, TCGA testing set, TCGA entire set, and GSE78229 dataset). Meanwhile, the area under curves (AUCs) of the risk signature for predicting 1-, 1.5-, 2-, 2.5-, and 3-year survival of PC patients were 0.802, 0.713, 0.676, 0.702, 0.777 in the TCGA training set, 0.790, 0.648, 0.698, 0. 772, 0.739 in TCGA testing set, 0.789, 0.690, 0.695, 0.733, 0.767 in TCGA entire set, and 0.550, 0.604, 0.774, 0.778, 0.860 in GSE78229 dataset, respectively (Fig. 2F–I).
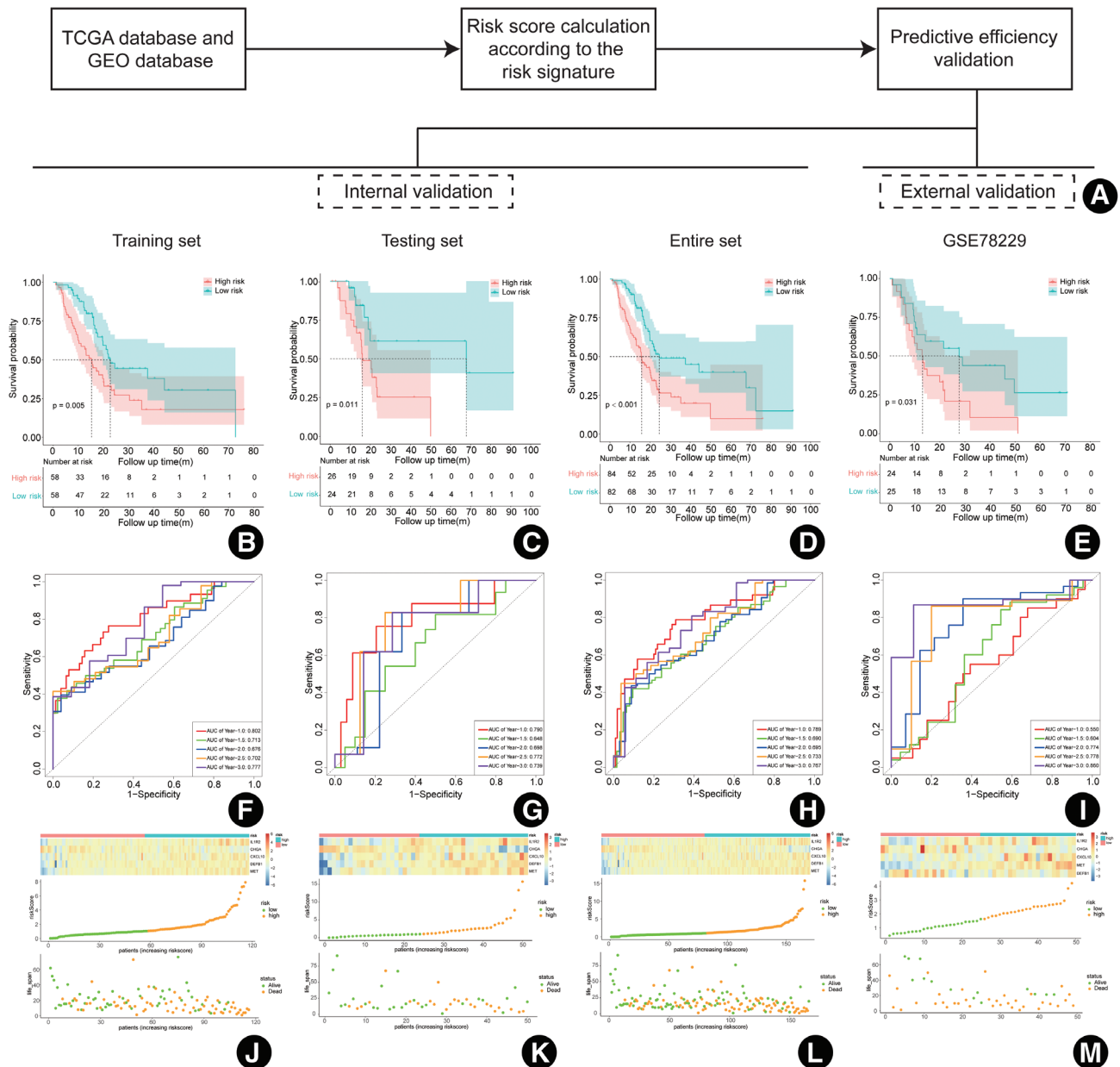
Figure 2. Effectiveness validation of the risk signature for survival prediction in training set, testing set, entire TCGA set, and GSE78229 set. (A) The process of the risk signature validation. (B–E) Kaplan-Meier analysis of OS of the risk signature in training set, testing set, entire TCGA set, and GSE78229 set. (F–I) Time-dependent ROC analysis of the risk signature in the 4 datasets. (J–M) Heatmap of the 5 hub genes expression, the risk scores distribution, and survival status plots of the patients in the 4 datasets. GEO = Gene Expression Omnibus, OS = overall survival, ROC = receiver operating characteristic, TCGA = The Cancer Genome Atlas.

Additionally, it was observed that as the risk score increased, the expression of CXCL10, DEFB1, IL1R2, and MET experienced a gradual increase, while the expression of CHGA experienced a stepwise decrease. Consistently, survival scatter plot indicated a significant increase in the number of deaths as the risk score rose (Fig. 2J–M). Overall, the above results further proved the effectiveness of the prediction signature in predicting the prognosis of PC, in which the overall survival (OS) of patients in the high-risk group is remarkably lower than that of patients in the low-risk group.

## Construction and validation of a nomogram based on the five-gene signature

To further optimize the prediction model, clinicopathological information was combined with the 5-gene signature to construct a nomogram, including gender, age, grade, AJCC_stage, T stage, and N stage (Fig. 3A, B). Finally, the risk score, age, and N stage were incorporated into the construction of the nomogram

based on univariate Cox regression analysis and multivariate Cox regression analysis (Fig. 3C).

Subsequently, calibration plot and time-dependent receiver operating characteristic (ROC) curve were applied to evaluate the effectiveness of the nomogram. The calibration curves presented satisfied coherence between predicted and actual 1-, 1.5-, and 2.0-year OS in TCGA training set, TCGA testing set, and TCGA entire set (Additional Figure S2A–C, http://links.lww.com/JP9/A52). Additionally, the AUCs of the risk signature for predicting 1.0-, 1.5-, and 2.0-year survival of PC patients were 0.766, 0.803, 0.804 in the TCGA training set, 0.677, 0.545, 0.692 in TCGA testing set and 0.741, 0.723, 0.773 in TCGA entire set (Fig. 3D–F). Both the validation models demonstrated the excellent performance of the nomogram in predicting the prognosis of PC.

IL1R2 was associated with poor prognosis of PC

Among the 5 genes in the prognostic signature, IL1R2 possessed a relatively high coefficient and hazard ratio (HR) value, which
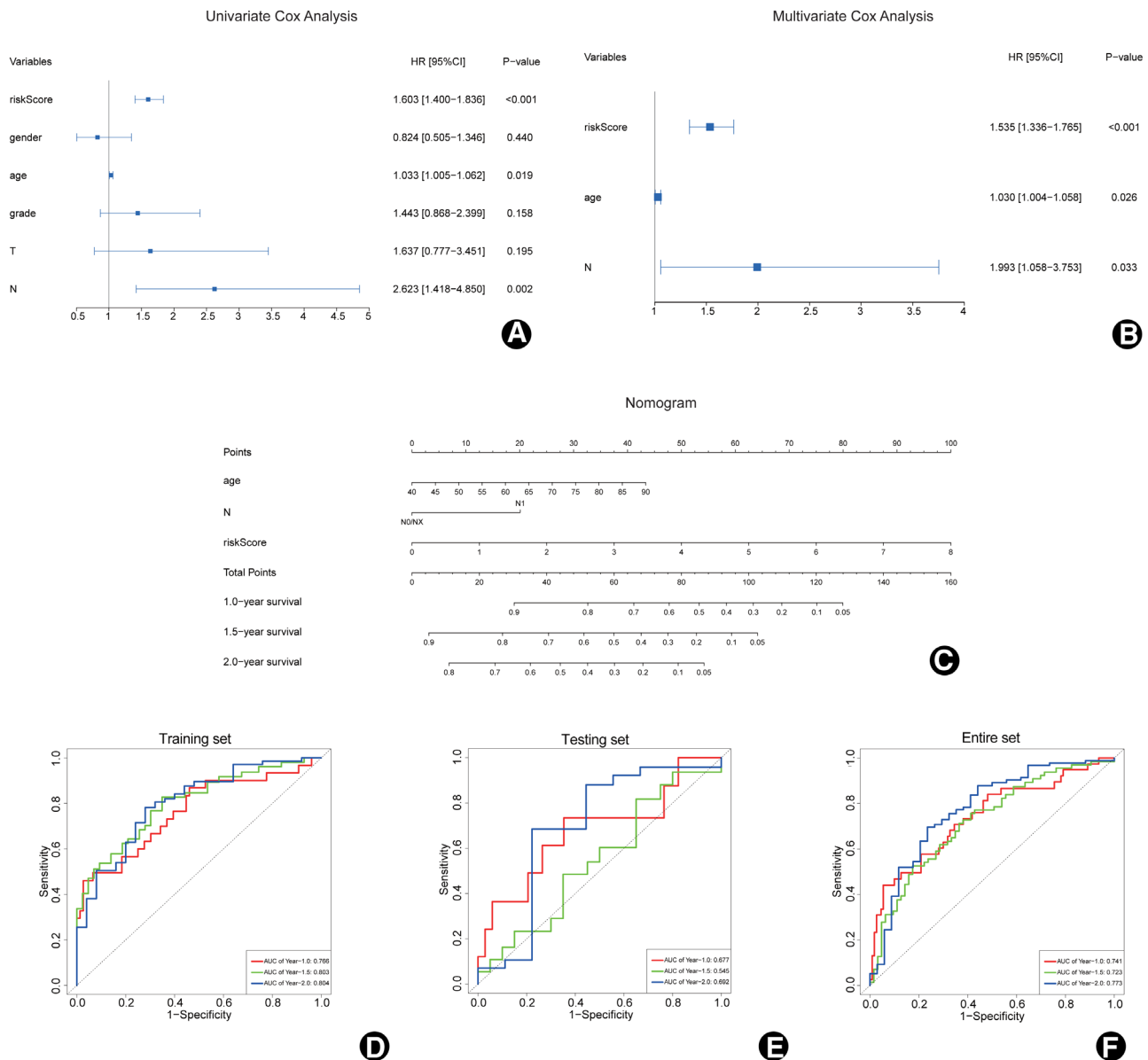
Figure 3. Nomogram construction for predicting 1-, 1.5- and 2.0-y survival rate of PC. (A, B) Univariate Cox regression analysis and multivariate Cox regression analysis in training set. (C) Nomogram integrating 4 IRGs-based risk score, age, and N stage. (D, F) Time-dependent ROC analysis of the nomogram in training set, testing set and entire set. IRG = immune-related gene, PC = pancreatic cancer.

made us consider that IL1R2 might play a pivotal role in predicting the prognosis of PC in the signature. Therefore, IL1R2 was paid special attention in the further exploration.

First, pan-cancer analysis of IL1R2 revealed that IL1R2 was lowly expressed in most tumor tissues and highly expressed only in PC and glioblastoma (Fig. 4A–C), which might be related to the unique tumor microenvironment of these 2 tumors. Meanwhile, IL1R2 was associated with higher tumor stage, higher grade, and higher T stage, but no significant association with N stage, age, and gender (Fig. 4D–I). In addition, based on the PC cell line data in the CCLE database, it was found that the expression of IL1R2 was positively correlated with the expression of PD-L1 (Fig. 4J, K), suggesting that high IL1R2 expression leading to poor prognosis of PC may be related to the immunosuppressive tumor microenvironment of PC.

IL1R2 promoted the proliferation, invasion, and metastasis of PC cells

In order to further explore why IL1R2 was associated with poor prognosis of PC, we first analyzed the single-cell dataset CRA001160, in which cancer cells were divided into IL1R2 low expression group and IL1R2 high expression group. DEGs analysis was performed, which found that MUC13, MUCL3, CCND2, and KRT13 were significantly upregulated in the cancer cells with high expression of IL1R2 (Fig. 5A), suggesting that IL1R2 might promote PC progression by promoting the proliferation, invasion, and migration ability of PC cells.

Additionally, molecular biology experiments were conducted to explore whether IL1R2 could affect biological behavior of PC cells. We first knocked down the expression of IL1R2 in T3M4 and BXPC-3 cell lines, respectively, and then measured
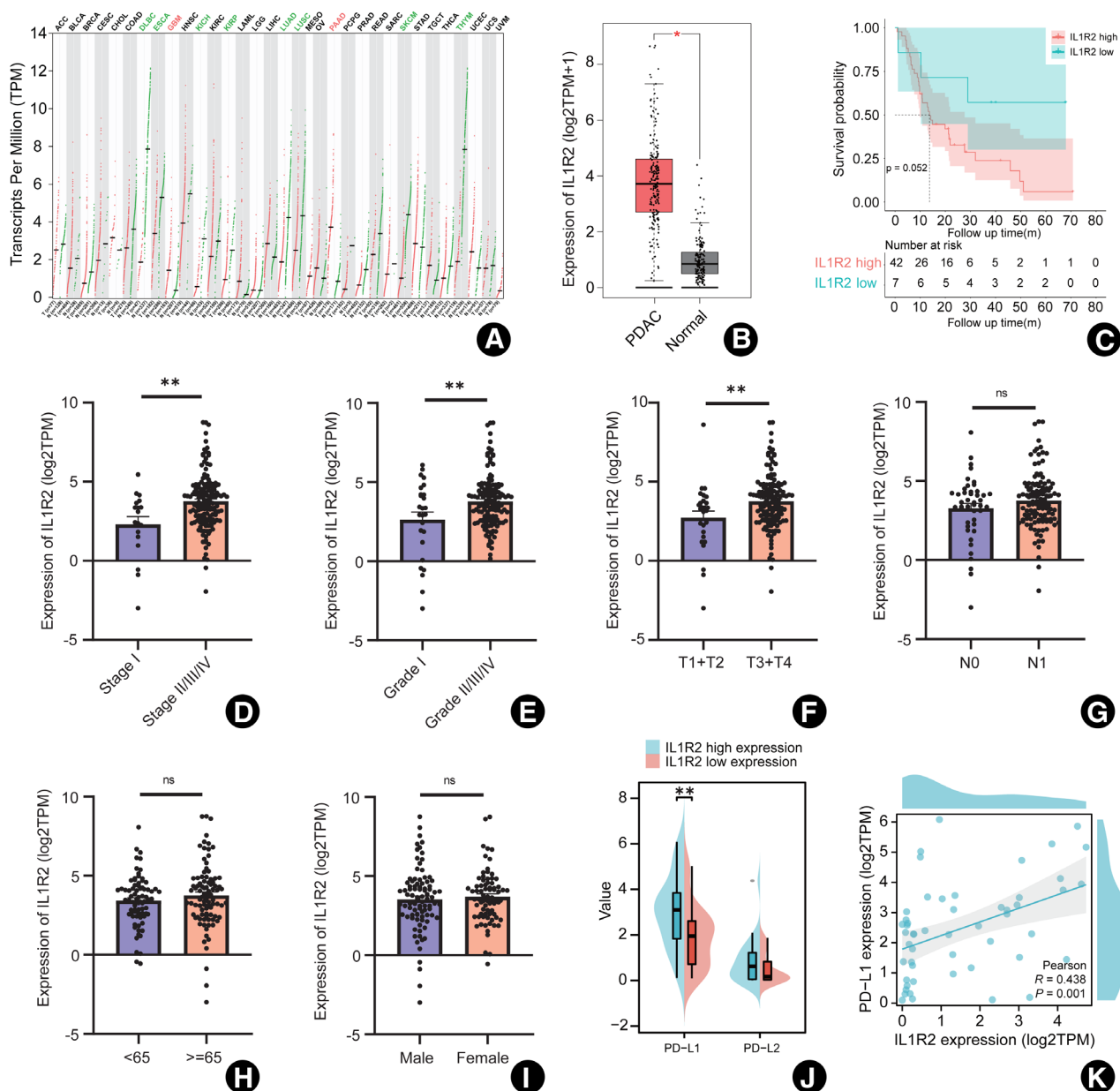
Figure 4. IL1R2 was significantly associated with poor prognosis of pancreatic cancer. (A) A pan-cancer analysis of IL1R2. Red represents a significant increase in tumor, green represents a significant decrease in tumor, and black represents no significant change. (B) Expression difference of IL1R2 between normal tissue and PC tissue according to RNA-seq data. (C) Kaplan-Meier analysis of OS between the high IL1R2 expression group and low IL1R2 expression group in GSE78229 dataset. (D–I) The correlation of IL1R2 expression with tumor grade, AJCC_stage, age, T stage, N stage and gender. (J, K) Correlation between expression of IL1R2 and PD-L1 in pancreatic cancer cell lines according to CCLE database. *$P < .05$; **$P < .01$. CCLE = Cancer Cell Line Encyclopedia, IL1R2 = interleukin 1 receptor type II, ns = no significance, OS = overall survival, PC = pancreatic cancer, PD-L1 = programmed cell death-ligand-1.
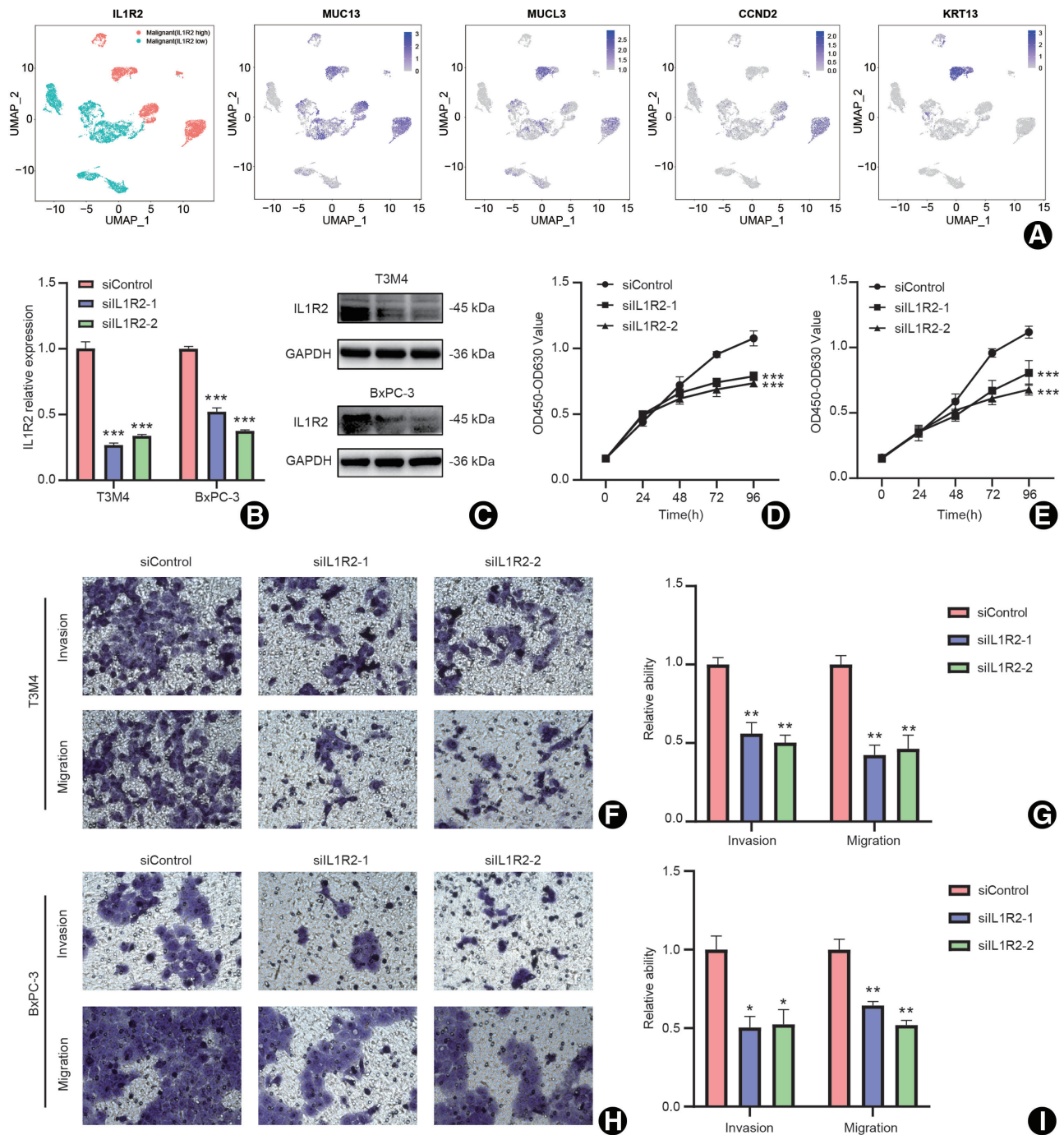
its proliferation, invasion, and migration ability (Fig. 5B, C). The results indicated that the proliferation, invasion, and migration ability of PC cells decreased significantly after IL1R2 knockdown (Fig. 5D–I), suggesting that IL1R2 was able to promote the proliferation, invasion, and migration ability of PC cells.

## IL1R2 predicted the immunosuppressive microenvironment of PC

Subsequently, DEGs analysis and functional enrichment were performed between IL1R2 high and low expression groups in

the TCGA dataset, which found that the immune-related signaling pathway was significantly downregulated in the IL1R2 high expression group (Fig. 6A, B). In addition, the ESTIMATE algorithm revealed that the immune infiltration scores were significantly decreased in the IL1R2 high expression group (Fig. 6C, D). Therefore, we hypothesized that the poor prognosis of PC due to IL1R2 might also be related to its effect on the immune microenvironment of PC.

Therefore, CIBERSORT algorithm was applied to calculate the proportion of immune cells in the tumor microenvironment of the patients in IL1R2 high expression group and IL1R2 low

Figure 5. IL1R2 was able to promote the proliferation, invasion, and migration ability of pancreatic cancer cell. (A) Expression of progression-related genes in pancreatic cancer cells with high or low IL1R2 expression in the single-cell dataset CRA001160. (B, C) Validation of IL1R2 knockdown efficiency in T3M4 cells and BxPC-3 cells. (D, E) CCK-8 assay of T3M4 cells and BxPC-3 cells after IL1R2 knockdown. (F–I) Invasion assays and migration assays of T3M4 cells and BxPC-3 cells after IL1R2 knockdown. *P < .05; **P < .01; ***P < .001. CCK-8 = Cell Counting Kit-8, IL1R2 = interleukin 1 receptor type II.
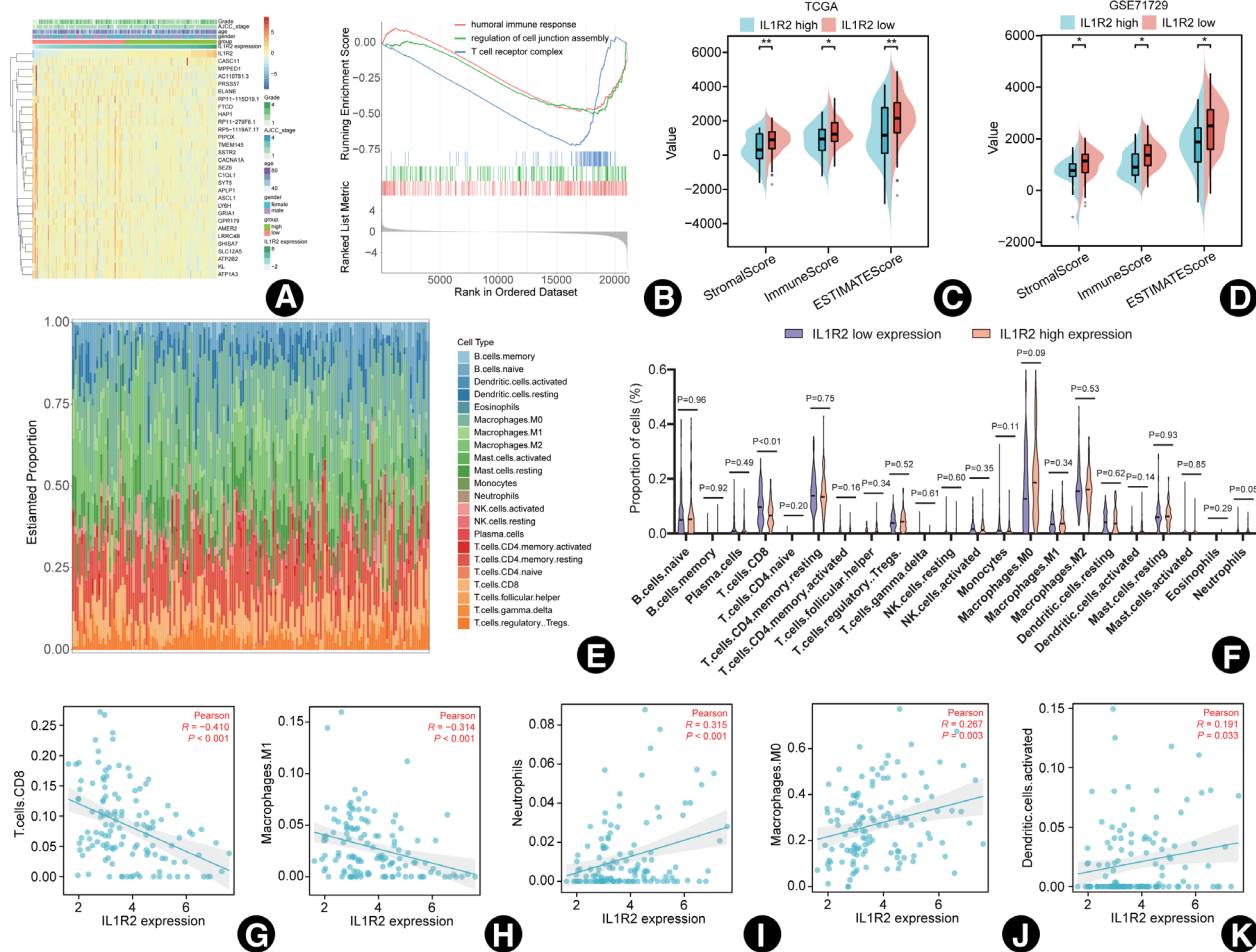
Figure 6. Immune cell infiltration difference between IL1R2 high and low expression groups. (A) Heatmap of top 30 DEGs in PC between IL1R2 high and low expression groups. (B) GSEA between IL1R2 high and low expression groups. (C, D) Immunity score obtained by ESTIMATE algorithm in high and low IL1R2 expression groups in TCGA dataset and GSE71729 dataset. (E, F) The abundance difference of the 22 types of immune cells between IL1R2 high and low expression groups. (G–K) Correlation analysis between the IL1R2 expression and the proportion of immune cells in GSE71729 dataset. Immune cell types with $P < .05$ were displayed. *$P < .05$; **$P < .01$. DEG = differentially expressed gene, GSEA = Gene Set Enrichment Analysis, IL1R2 = interleukin 1 receptor type II, PC = pancreatic cancer, TCGA = The Cancer Genome Atlas.

expression group, respectively (Fig. 6E). It was discovered that CD8+ T cell infiltration was significantly decreased in the IL1R2 high expression group (Fig. 6F). Consistently, the analysis of GSE71729 dataset showed that IL1R2 was significantly negatively correlated with CD8+ T cells, M1 macrophages, while remarkably positively associated with neutrophils, M0 macrophages, and activated dendritic cells (Fig. 6G–K). Combined with the results that the expression of IL1R2 was positively correlated with the expression of PD-L1 (Fig. 4J–K), we made hypothesis that high IL1R2 expression leading to poor prognosis of PC may be related to the immunosuppressive tumor microenvironment of PC.

Single-cell sequencing analysis showed interaction between IL1R2 high expression PC cells and CD8+T cells in tumor microenvironment of PC

To further validate the above results, the single-cell dataset CRA001160 was accessed and analyzed. First, CRA001160 dataset was divided into 10 cell clusters by dimensional reduction clustering (Fig. 7A), in which we extracted epithelial cells and performed further analysis. By dimensional reduction clustering, it was found that there were significant differences between PC cells and normal ductal cells (Fig. 7B), and the expression of IL1R2 was significantly higher in PC cells than in normal ductal cells (Fig. 7C).

Subsequently, the patients in CRA001160 were divided into IL1R2 high expression group, median expression group, and low expression group according the expression of IL1R2 in cancer cells of each patient (Fig. 7D). It was found that the infiltration of CD8+ T cells was significantly higher in patients in IL1R2 low expression group than in IL1R2 high expression group (Fig. 7E), suggesting that high expression of IL1R2 in cancer cells might inhibit CD8+ T cell infiltration in PC microenvironment. To explore the underlying mechanisms in depth, the CellChat algorithm was applied to explore potential interactions pathways between cells (Fig. 7F), resulting in significant differences between the effects of IL1R2 high expression cancer cell and IL1R2 low expression cancer cells on various types of immune cells (Fig. 7G–J).

IL1R2 was able to predict the efficacy of immunotherapy for PC

The results above proved that IL1R2 may be related to the immunosuppressive microenvironment in PC. Next, we wondered whether IL1R2 was able to predict immunotherapy efficacy in patients with PC. Due to the high correlation between TMB and tumor immunotherapy efficacy, mutation profiles of both the IL1R2 high expression group and low expression group were analyzed and visualized. For the IL1R2
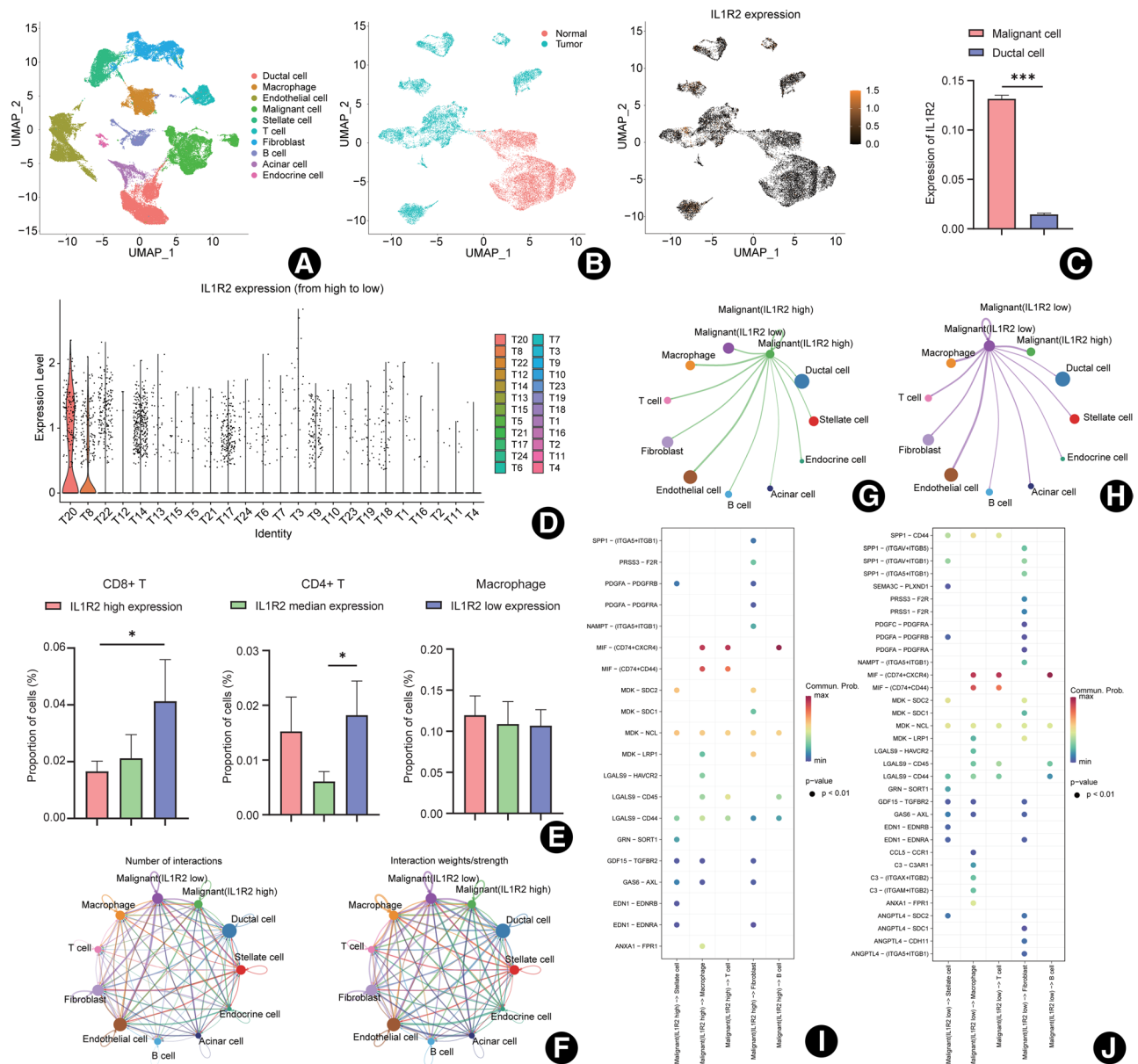
Figure 7. Analysis of IL1R2 expression and immune cell infiltration in single-cell dataset CRA001160. (A) The UMAP plots of diverse cell types in CRA001160 colored by major cell lineage. (B) The UMAP plots of epithelial cells in CRA001160. (C) Comparison of IL1R2 expression in normal ductal and PC cells. (D) Relative expression of IL1R2 in cancer cells of each patient (ranked from high to low). (E) Comparison of infiltration of CD8+T cells, CD4+T cells, and macrophages in IL1R2 high, medium and low expression group. (F–J) Interactions between tumor cells with high or low IL1R2 expression and cells in the tumor microenvironment and their potential pathways in the single-cell dataset CRA001160. *$P < .05$; ***$P < .001$. IL1R2 = interleukin 1 receptor type II, PC = pancreatic cancer, UMAP = Uniform Manifold Approximation and Projection.

high expression group, the genes with the highest mutation rate were *KRAS*, *TP53*, *SMAD4*, *CDKN2A*, *TTN*, *RNF43*, *FLG*, *PEG3*, *ADAMTS12*, and *NTF3* (Fig. 8A). And for the IL1R2 low expression group, the top 10 frequently mutation genes were *KRAS*, *TP53*, *SMAD4*, *TTN*, *CDKN2A*, *MUC16*, *DNAH11*, *GNAS*, *HECW2*, and *RNF213* (Fig. 8B). Notably, the mutation frequency of the 4 driver genes of PC, *KRAS*, *TP53*, *SMAD4*, and *CDKN2A*, were all significantly elevated in the IL1R2 high expression group (Fig. 8C, 86%: 68% for *KRAS*, 73%: 60% for *TP53*, 25%: 22% for *SMAD4*, 22%: 12% for *CDKN2A*).

Additionally, it was found that patients with high IL1R2 expression possessed higher TMB (Fig. 8D), although there was no significant correlation between TMB and patients' prognosis (Fig. 8E). Furthermore, according to the comprehensive

analysis of IL1R2 expression and IPS algorithm, patients with high expression of IL1R2 were more likely to benefit from anti-PD-1 therapy, anti-CTLA-4 therapy, and the combination of anti-PD-1 and anti-CTLA-4 therapy (Fig. 8F–K). Therefore, IL1R2 is expected to be one of the biomarkers to predict the efficacy of immunotherapy for PC.

Discussion

PC is a highly malignancy with an extremely poor prognosis,[29] and a crucial reason for the dismal status is the lack of reliable prognostic signature and biomarkers. Therefore, we constructed an accurate immune-related prognostic signature of PC and the corresponding nomogram in this study. In the prognostic signature, CHGA CXCL10, DEFB1, and MET were demonstrated
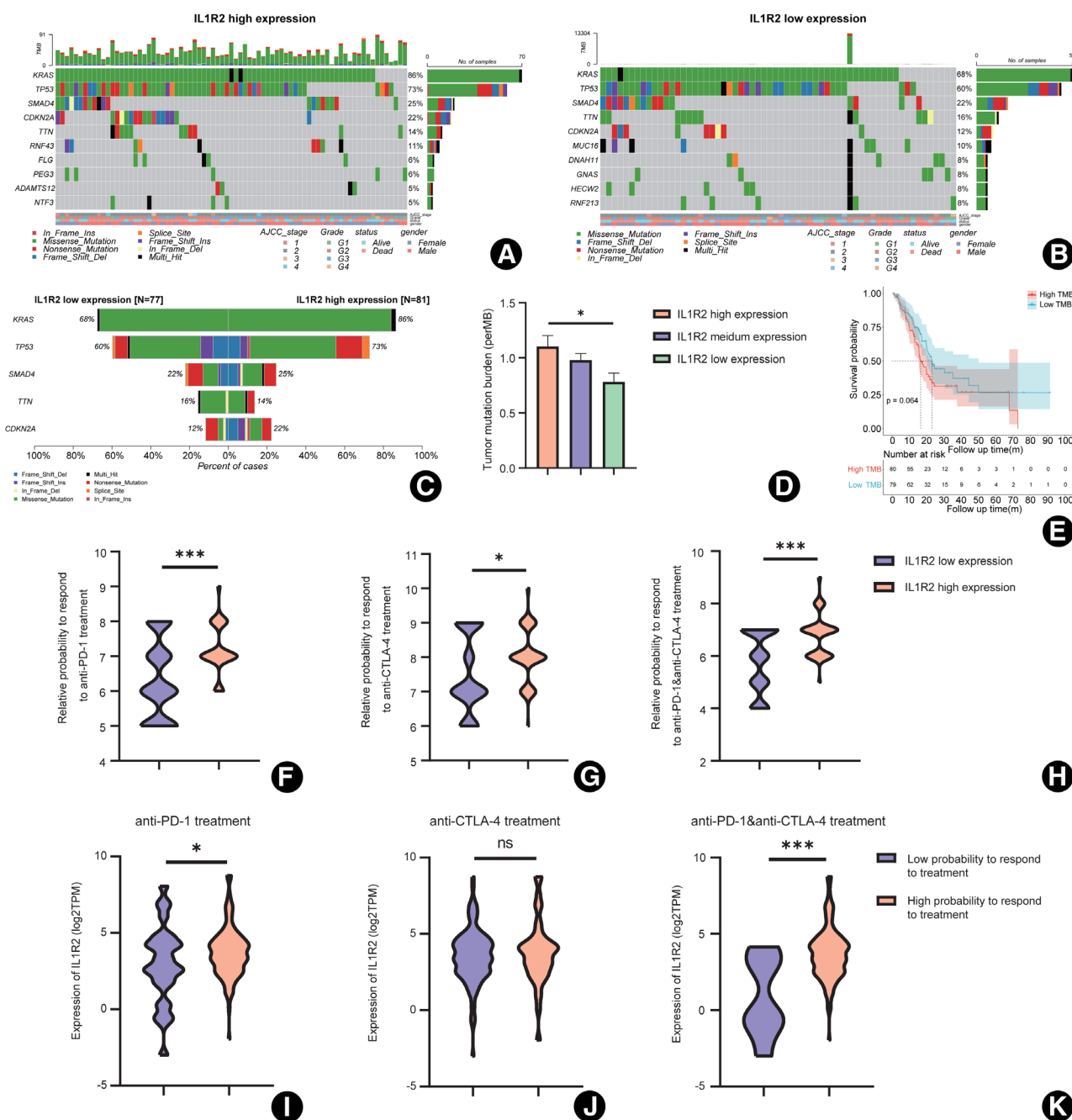
Figure 8. IL1R2 was able to serve as a biomarker to predict the efficacy of immunotherapy for pancreatic cancer. (A, B) Mutation profile of PC patients in IL1R2 high expression group and low expression group. (C) Mutation rate comparison of genes with high mutation rate between IL1R2 high and low expression group. (D) The comparison of TMB between IL1R2 high, median, and low expression groups. (E) Kaplan-Meier analysis of OS between high and low TMB group. (F–K) The relationship between IL1R2 expression and the relative probabilities of responding to immunotherapy, including anti-PD-1 therapy, anti-CTLA-4 therapy, and the combination therapy. $*P < .05$; $***P < .001$. IL1R2 = interleukin 1 receptor type II, OS = overall survival, PC = pancreatic cancer, TMB = tumor mutation burden.

to be involved in cancer proliferation, metastasis, chemoresistance, and immune microenvironment.[30–35] However, the role of IL1R2 in PC development has not been reported yet. Considering its high coefficient and HR value in the prognostic signature of PC, we next further explored the role of IL1R2 in PC development and its in-depth mechanism.

IL1R2 was a decoy receptor of interleukin-1 (IL-1), which acted as a competitive inhibitor of IL-1 and prevented its binding to IL1R1, blocking the IL1β signaling in inflammation diseases.[36,37] In addition, it was also reported that IL1R2 was able to act as an intracellular inhibitor for pro-IL1α in necrosis-induced sterile inflammation.[38] At the same time, some studies

have preliminarily identified the role of IL1R2 in the development of cancers. Mar et al[39] found that intracellular IL1R2 was able to acts with c-Fos to enhance the transcription of IL-6 and vascular endothelial growth factor (VEGF)-A, which promoted angiogenesis in colon cancer cells. And blocking IL1R2 with neutralizing antibody was proved to inhibit breast cancer progression by targeting breast tumor initiating cells.[40] However, the role of IL1R2 in the development of PC, including its own oncogenic potential and its effect on the microenvironment of PC, has not been reported yet.

In this project, IL1R2 was identified as a pivotal factor in the progression of PC, which was significantly associated with

higher stage, higher grade, and higher T stage. Meanwhile, knockdown of IL1R2 inhibited the proliferation, invasion, and migration of PC cell lines, suggesting that IL1R2 itself was able to promote the progression of PC by promoting the proliferation and metastasis of PC. And the results were consistent with the previous results in other cancers.[41]

Meanwhile, as patients with IL1R2 high expression presented an immunosuppressive tumor microenvironment, such as fewer CD8+ T cells and M1-type macrophages, both of which have been reported to exhibit pronounced anti-tumor effects.[42,43] Additionally, based on cell line transcriptomic data from the CCLE database, it was found that the expression of IL1R2 in PC cells was positively correlated with the expression of PD-L1, suggesting that PC cells might suppress the activation of CD8+ T cells by upregulating PD-L1 on the cell membrane surface,[44,45] resulting in an immunosuppressive tumor microenvironment. According to previous studies, we found that IL1R2 was able to promote the expression of hypoxia-inducible factor (HIF)1α,[46] which was one of the key factors in the formation of immune suppressive tumor microenvironment.[47] Therefore, we considered that the IL1R2-HIF1α axis was one of the mechanisms of the reduction of CD8+T cells in the PC microenvironment.

Finally, since we have demonstrated the strong association of IL1R2 expression with the immune microenvironment of PC, we next wondered whether IL1R2 expression could predict the efficacy of immunotherapy for PC. First, it was found that the mutation frequency of all 4 driver genes of PC (KRAS, TP53, CDKN2A, SMAD4) were significantly elevated in the IL1R2 high expression group. Additionally, TMB, a biomarker closely associated with improved immunotherapies,[48] was proved to be increased in the IL1R2 high expression group. Combined with the IPS algorithm, it was found that patients in IL1R2 high expression possessed a relatively higher probability of responding to anti-PD1 therapy, anti-CTLA4 therapy and the combination of anti-PD1 and anti-CTLA-4 therapy.

Conclusions

In conclusion, an immune-related prognostic signature and the corresponding nomogram for PC were established and validated in different datasets. Furthermore, IL1R2 was identified as the gene occupying the most paramount position in the risk signature. IL1R2 was significantly associated with poor prognosis of PC and was proved to promote the progression of PC by promoting the proliferation, invasion, and migration of PC cells. Meanwhile, both single-cell analysis and bulk-seq analysis demonstrated that the expression of IL1R2 may be associated with decreased infiltration of CD8+ T cells in PC microenvironment, which might result from the high expression of PD-L1 in IL1R2-high expressing PC cells. Finally, it was demonstrated that patients with high IL1R2 expression possessed a higher TMB and higher probability to benefit from immunotherapy, suggesting that IL1R2 was able to serve as a potential biomarker for predicting PC immunotherapy efficiency.

Acknowledgments

Author contributions

Financial support

Conflicts of interest

YZ is the Editorial Board member of Journal of Pancreatology. CW is the managing editor of Journal of Pancreatology. They were blinded from reviewing or making decisions on the manuscript. The article was subject to the journal's standard procedures, with peer review handled independently of this Editorial Board member and their research groups. The other authors declare that they have no conflicts of interest.

Ethics approval

The Ethics Committee of PUMCH approved the study (No. I-22PJ984) on December 8th, 2022 and the patients were exempted from informed consent.

Declaration of participant consent

Not applicable.

References

[1] Siegel RL, Miller KD, Wagle NS, et al. Cancer statistics, 2023. CA Cancer J Clin. 2023;73:17–48.

[2] Klein AP. Pancreatic cancer epidemiology: understanding the role of lifestyle and inherited risk factors. Nat Rev Gastroenterol Hepatol. 2021;18:493–502.

[3] Kleeff J, Korc M, Apte M, et al. Pancreatic cancer. Nat Rev Dis Primers. 2016;2:16022.

[4] Iacobuzio-Donahue CA. The war on pancreatic cancer: progress and promise. Nat Rev Gastroenterol Hepatol. 2023;20:75–76.

[5] Stoffel EM, Brand RE, Goggins M. Pancreatic cancer: changing epidemiology and new approaches to risk assessment, early detection, and prevention. Gastroenterology. 2023;164:752–765.

[6] Fu T, Dai L-J, Wu S-Y, et al. Spatial architecture of the immune microenvironment orchestrates tumor immunity and therapeutic response. J Hematol Oncol. 2021;14:98.

[7] Kao KC, Vilbois S, Tsai C-H, et al. Metabolic communication in the tumour-immune microenvironment. Nat Cell Biol. 2022;24:1574–1583.

[8] Gao A, Liu X, Lin W, et al. Tumor-derived ILT4 induces T cell senescence and suppresses tumor immunity. J ImmunoTher Cancer. 2021;9:e001536.

[9] Zhang Y, Fan Y, Jing X, et al. OTUD5-mediated deubiquitination of YAP in macrophage promotes M2 phenotype polarization and favors triple-negative breast cancer progression. Cancer Lett. 2021;504:104–115.

[10] Bhattacharya S, Andorf S, Gomes L, et al. ImmPort: disseminating data to the public for the future of immunology. Immunol Res. 2014;58:234–239.

[11] Yang S, He P, Wang J, et al. A novel MIF signaling pathway drives the malignant character of pancreatic cancer by targeting NR3C2. Cancer Res. 2016;76:3838–3850.

[12] Wang J, Yang S, He P, et al. Endothelial nitric oxide synthase traffic inducer (NOSTRIN) is a negative regulator of disease aggressiveness in pancreatic cancer. Clin Cancer Res. 2016;22:5992–6001.

[13] Moffitt RA, Marayati R, Flate EL, et al. Virtual microdissection identifies distinct tumor- and stroma-specific subtypes of pancreatic ductal adenocarcinoma. Nat Genet. 2015;47:1168–1178.

[14] Sun D, Wang J, Han Y, et al. TISCH: a comprehensive web resource enabling interactive single-cell transcriptome visualization of tumor microenvironment. Nucleic Acids Res. 2021;49:D1420–D1430.

[15] Peng J, Sun B-F, Chen C-Y, et al. Single-cell RNA-seq highlights intra-tumoral heterogeneity and malignant progression in pancreatic ductal adenocarcinoma. Cell Res. 2019;29:725–738.

[16] Barretina J, Caponigro G, Stransky N, et al. The cancer cell line encyclopedia enables predictive modelling of anticancer drug sensitivity. Nature. 2012;483:603–607.

[17] Ritchie ME, Phipson B, Wu D, et al. Limma powers differential expression analyses for RNA-sequencing and microarray studies. Nucleic Acids Res. 2015;43:e47.

[18] Harris MA, Clark J, Ireland A, et al. The gene ontology (GO) database and informatics resource. Nucleic Acids Res. 2004;32:D258–D261.

[19] Kanehisa M, Goto S. KEGG: Kyoto encyclopedia of genes and genomes. Nucleic Acids Res. 2000;28:27–30.

[20] Newman AM, Liu CL, Green MR, et al. Robust enumeration of cell subsets from tissue expression profiles. Nat Methods. 2015;12:453–457.

[21] Yoshihara K, Shahmoradgoli M, Martínez E, et al. Inferring tumour purity and stromal and immune cell admixture from expression data. Nat Commun. 2013;4:2612.

[22] Mayakonda A, Lin D-C, Assenov Y, et al. Maftools: efficient and comprehensive analysis of somatic variants in cancer. Genome Res. 2018;28:1747–1756.

[23] Charoentong P, Finotello F, Angelova M, et al. Pan-cancer immunogenomic analyses reveal genotype-immunophenotype relationships and predictors of response to checkpoint blockade. Cell Rep. 2017;18:248–262.

[24] Wang C, Chen Y, Xinpeng Y, et al. Construction of immune-related signature and identification of S100A14 determining immune-suppressive microenvironment in pancreatic cancer. BMC Cancer. 2022;22:879.

[25] Wang C, Zhang T, Liao Q, et al. Metformin inhibits pancreatic cancer metastasis caused by SMAD4 deficiency and consequent HNF4G upregulation. Protein Cell. 2021;12:128–144.

[26] Ren B, Yang J, Wang C, et al. High-resolution Hi-C maps highlight multiscale 3D epigenome reprogramming during pancreatic cancer metastasis. J Hematol Oncol. 2021;14:120.

[27] Chen P, He Z, Wang J, et al. Hypoxia-Induced ZWINT mediates pancreatic cancer proliferation by interacting with p53/p21. Front Cell Dev Biol. 2021;9:682131.

[28] Song J, Ruze R, Chen Y, et al. Construction of a novel model based on cell-in-cell-related genes and validation of KRT7 as a biomarker for predicting survival and immune microenvironment in pancreatic cancer. BMC Cancer. 2022;22:894.

[29] Wood LD, Canto MI, Jaffee EM, et al. Pancreatic cancer: pathogenesis, screening, diagnosis, and treatment. Gastroenterology. 2022;163:386–402.e1.

[30] Zhang X, Zhang H, Shen B, et al. Chromogranin-a expression as a novel biomarker for early diagnosis of colon cancer patients. Int J Mol Sci. 2019;20:2919.

[31] Hirth M, Gandla J, Höper C, et al. CXCL10 and CCL21 promote migration of pancreatic cancer cells toward sensory neurons and neural remodeling in tumors in mice, associated with pain in patients. Gastroenterology. 2020;159:665–681.e13.

[32] Limagne E, Nuttin L, Thibaudin M, et al. MEK inhibition overcomes chemoimmunotherapy resistance by inducing CXCL10 in cancer cells. Cancer Cell. 2022;40:136–152.e12.

[33] Lee M, Wiedemann T, Gross C, et al. Targeting PI3K/mTOR signaling displays potent antitumor efficacy against nonfunctioning pituitary adenomas. Clin Cancer Res. 2015;21:3204–3215.

[34] Recondo G, Che J, Jänne PA, et al. Targeting MET dysregulation in cancer. Cancer Discov. 2020;10:922–934.

[35] Guo R, Luo J, Chang J, et al. MET-dependent solid tumours—molecular diagnosis and targeted therapy. Nat Rev Clin Oncol. 2020;17:569–587.

[36] Molgora M, Supino D, Mantovani A, et al. Tuning inflammation and immunity by the negative regulators IL-1R2 and IL-1R8. Immunol Rev. 2018;281:233–247.

[37] Garlanda C, Riva F, Bonavita E, et al. Negative regulatory receptors of the IL-1 family. Semin Immunol. 2013;25:408–415.

[38] Zheng Y, Humphry M, Maguire JJ, et al. Intracellular interleukin-1 receptor 2 binding prevents cleavage and activity of interleukin-1α, controlling necrosis-induced sterile inflammation. Immunity. 2013;38:285–295.

[39] Mar AC, Chu C-H, Lee H-J, et al. Interleukin-1 receptor type 2 acts with c-Fos to enhance the expression of interleukin-6 and vascular endothelial growth factor A in colon cancer cells and induce angiogenesis. J Biol Chem. 2015;290:22212–22224.

[40] Zhang L, Qiang J, Yang X, et al. IL1R2 blockade suppresses breast tumorigenesis and progression by impairing USP15-dependent BMI1 stability. Adv Sci (Weinh). 2020;7:1901728.

[41] Liu Y, Xing Z, Yuan M, et al. IL1R2 promotes tumor progression via JAK2/STAT3 pathway in human clear cell renal cell carcinoma. Pathol Res Pract. 2022;238:154069.

[42] van Vlerken-Ysla L, Tyurina YY, Kagan VE, et al. Functional states of myeloid cells in cancer. Cancer Cell. 2023;41:490–504.

[43] Johnson DB, Balko JM. T cell dynamism and immune-related adverse events. Cancer Cell. 2023;41:658–659.

[44] Wang Y, Zhou S-K, Wang Y, et al. Engineering tumor-specific gene nanomedicine to recruit and activate T cells for enhanced immunotherapy. Nat Commun. 2023;14:1993.

[45] Yi M, Zheng X, Niu M, et al. Combination strategies with PD-1/PD-L1 blockade: current advances and future directions. Mol Cancer. 2022;21:28.

[46] Zhou N, Liu L, Li Q. IL1R2 promotes retinal angiogenesis to participate in retinopathy of prematurity by activating the HIF1α/PFKFB3 pathway. Exp Eye Res. 2023;239:109750.

[47] Wu Q, Li Y, Nepovimova E, et al. Hypoxia-inducible factors: master regulators of hypoxic tumor immune escape. J Hematol Oncol. 2022;15:77.

[48] Mayoh C, Gifford AJ, Terry R, et al. A novel transcriptional signature identifies T-cell infiltration in high-risk paediatric cancer. Genome Med. 2023;15:20.